

Acrosin structure-based design, synthesis and biological activities of 7-azaindol derivatives as new acrosin inhibitors

Jun Hang Jiang¹, Xue Fei Liu¹, Can Hui Zhen, You Jun Zhou,
Ju Zhu, Jia Guo Lv^{*}, Chun Quan Sheng

Department of Medicinal Chemistry, School of Pharmacy, Second Military Medical University, Shanghai 200433, China

Received 8 June 2010

Available online 22 December 2010

Abstract

A series of 7-azaindol derivatives were designed based on the homologous 3D model of human acrosin. These compounds were synthesized and evaluated for their human acrosin inhibitory activities *in vitro*. Compounds **7a**, **7i**, **7j**, **7k** and **7n** showed highly inhibitory activity against human acrosin. The three-dimensional structure–activity relationship was investigated through a CoMFA model, which provided valuable information to further study of potential human acrosin inhibitors.

© 2010 Published by Elsevier B.V. on behalf of Chinese Chemical Society.

Keywords: Rational design; Azaindole; Synthesis; Acrosin; CoMFA

Acrosin is a multifunctional protein located in acrosome. It not only affects motility of sperm but also disperses acrosomal matrix and hydrolyzes the zona pellucida, which helps sperm enter and fusion to ovum. Therefore contraception can be achieved through acrosome enzyme inhibition. In recent years, acrosin has become an attractive target in contraceptive drug discovery [1].

In our previous studies, the homologous 3D model of human acrosin was built based on the crystal structures of ram and boar acrosins [2], and the active site was searched by Insight II/binding site analysis. On the basis of these studies, we further analyzed the properties of the active site by the multiple copy simultaneous search (MCSS) method [3]. It was demonstrated that the active site of human acrosin is an irregular groove, which could be divided into three subsites (P1, P2 and G) [4].

We have found that lonidamine, an antineoplastic agent with indazole skeleton, had anti-acrosin activity *in vitro* [5]. Based on the principle of bioisosterism, a series 7-azaindol compounds were designed in the present study. The binding mode of azaindole was further investigated using the docking program Autodock (Fig. 1) [6]. The results showed that azaindole could be well accommodated by the active site of human acrosin. The azaindole ring resided at the entrance of the P1 subsite, which supported the whole structure through the hydrophobic interaction with the residues Val245 and Gly246. The 3-ethylester group was located in the P1 subsite, forming hydrogen-bonds with the key residue Gln218. Other 1-substituents were extended to the P2 subsite, which were surrounded by a hydrophobic

* Corresponding authors.

E-mail addresses: ljj20060508@yahoo.com.cn (J.G. Lv), shengcq@hotmail.com (C.Q. Sheng).

¹ Co-first author.

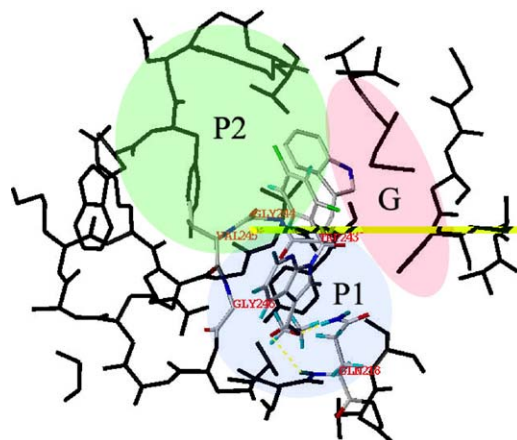
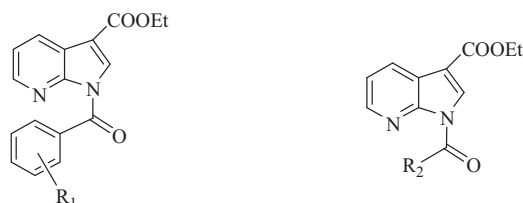


Fig. 1. Binding model of 7-azaindole with the active site residues of human acrosin.

center lined with the residues Val245, Gly244 and Trp243. Therefore, we synthesized a series of 7-azaindol derivatives and tested their biological activities.

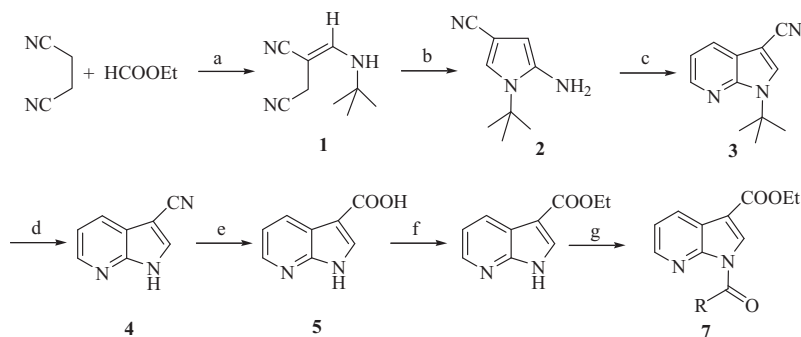
The chemical structures and synthetic route of the azaindole derivatives were depicted in Fig. 2 and Scheme 1. Succinonitrile, ethyl formate and *t*-butylamine were condensed to afford compound **1**, which was subsequently converted to compound **2** by ring closure reaction. Cyclization reaction of **2** with 1,1,3,3-tetramethoxypropane formed compound **3** [7]. De-*tert*-butylation of **3** provided compound **4**, which was hydrolyzed to get compound **5**. Intermediate **5** was condensed to yield compound **6**. Acylation of **6** provided the target compounds **7** [8].

Preliminary *in vitro* acrosin inhibitory activity of the novel compounds was shown in Table 1. The data demonstrated that most of the compounds had potent *in vitro* acrosin inhibitory activity. So we further investigate their anti-acrosin activity (Table 2). The result showed that compounds **7a**, **7i**, **7j**, **7k** and **7n** showed highly stronger anti-acrosin activity



7a: R₁ = H; **7b**: R₁ = 2-F; **7c**: R₁ = 3-F; **7d**: R₁ = 2-Cl; **7e**: R₁ = 2-CH₃; **7f**: R₁ = 2-CH₃O; **7g**: R₁ = 2-CH₃O, 4-CH₃O; **7h**: R₁ = 2-Cl, 6-Cl; **7i**: R₁ = 2-Cl, 4-Cl; **7j**: R₁ = 2-Cl, 4-F; **7k**: R₁ = 2-Br, 4-F; **7l**: R₁ = 3-Cl, 4-Cl; **7m**: R₂ = 2,4-dichloro-1-benzyl; **7n**: R₂ = 2-thienyl.

Fig. 2. Compounds with azaindole ring.



Scheme 1. Synthesis of compounds **7a–7n**. Reagents and conditions: (a) NaH, *t*-butylamine, reflux, 5hr; (b) KOH, EtOH; (c) 1,1,3,3-tetramethoxypropane, toluene, *p*-TosOH, 95 °C; (d) AlCl₃, xylene, reflux, 8hr; (e) HCl, 70 °C; (f) condensing agent EDC, EtOH, 50 °C; (g) NaH, substituted acyl chloride.

Table 1

Preliminary anti-acrosin activity data of the target compounds at concentration of 60 $\mu\text{mol/mL}$.

Compounds	Acrosin activity ^a (IU/ 10^6 sperm)	Inhibition ratio ^b
7a	-12.768	1.190
7b	18.424	0.727
7c	7.567	0.888
7d	31.334	0.535
7e	67.254	0.002
7f	52.969	0.214
7g	16.978	0.748
7h	62.181	0.077
7i	2.619	0.961
7j	0.780	0.988
7k	-8.337	1.124
7l	-4.606	1.068
7m	3.619	0.946
7n	-11.676	1.173

^a Standard activity is 67.376 IU/ 10^6 Sperm.^b Inhibition ratio = (standard activity - experimental activity)/standard activity.

Table 2

In vitro inhibitory activities of human acrosin.

Compounds	IC ₅₀ ($\mu\text{mol/mL}$)
7a	2.21
7i	0.29
7j	3.47
7k	1.74
7n	3.15
TLCK	142.6

than the standard control compound TLCK (*N*-tosyl-L-lysine chloromethyl ketone). Then we performed a CoMFA research (except compound **7m**) to establish the 3D-QSAR model based on the data of activity (Fig. 3). The CoMFA result ($q^2 = 0.516$, $r^2 = 0.776$, $\text{SEE} = 0.300$, $F = 19.044$, $n = 2$, steric and electronic field contribution were 0.279 and 0.721, respectively) indicated that electron-withdrawing group was favorable in the region of position C-2 at the benzene ring (blue part), and large group was unfavorable in the region of position C-4 at the benzene ring (yellow part). The docking model also revealed that small groups were beneficial to be stretched into the P2 subsite, which was in accordance with the CoMFA results. The anti-acrosin activity data demonstrated that halogens at position C-2 and C-4 of the benzene ring were more favorable for the inhibitory activity than the methoxyl group, which was in consistency with the CoMFA results. The bioassay results also hinted that the parent scaffold of these compounds could play an important role in the inhibition of human acrosin.

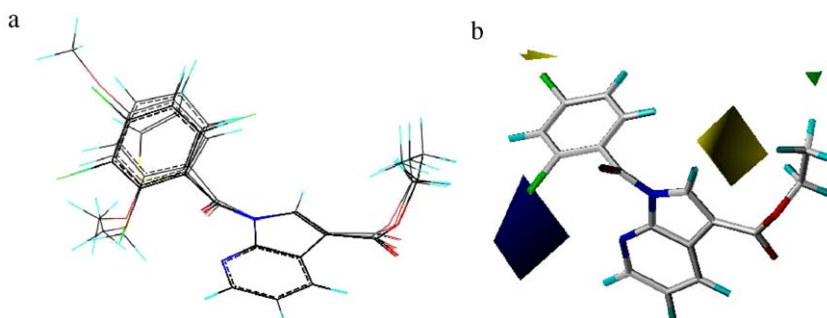


Fig. 3. (a) Superposition of the compounds **7a–7l**, and **7n**. (b) Steric (yellow and green part) and electronic (blue part) field of CoMFA model. (For interpretation of the references to color in this figure legend, the reader is referred to the web version of the article.)

In summary, the novel 7-azaindol derivatives were designed and synthesized and their anti-acrosin activity *in vitro* were tested. The result showed that compound **7i** had the highest activity. Subsequently, we built a CoMFA model to help us to discuss the three-dimensional structure–activity relationship to guide further structure modification.

Acknowledgments

This work was supported by the Shanghai Family Planning Commission Research Fund (No. 2007JG02) and Shanghai Leading Academic Discipline Project (No. B906).

References

- [1] R. Tranter, J.A. Read, R. Jones, et al. *J. Structure* 8 (2000) 1179.
- [2] J.G. Lv, C.Q. Sheng, M. Zhang, et al. *Acta Chim. Sin.* 64 (2006) 1073.
- [3] A. Caflich, A. Miranker, M. Karplus, *J. Med. Chem.* 36 (1993) 2142–2167.
- [4] J. Zhang, C.H. Zheng, C.Q. Sheng, et al. *Chem. J. Chin. Univ.* 30 (2009) 2409.
- [5] M.E. Traina, M. Guarino, A. Natoli, et al. *Toxicol. Appl. Pharm.* 221 (2007) 95.
- [6] G.M. Morris, D.S. Goodsell, R.S. Halliday, et al. *J. Comput. Chem.* 19 (1998) 1639.
- [7] A. Marcello, A. Roberto, C.M. Candida, et al. *Org. Proc. Res. Dev.* 7 (2003) 209.
- [8] Yield, physical and spectral data for some synthesized compounds: **7a** Full yield 95.0%, mp: 137–138 °C. ¹H NMR (300 MHz, CDCl₃): δ 1.41–1.46(t, 3H, *J* = 7.2 Hz), 4.39–4.46(q, 2H, *J* = 7.2 Hz), 7.26–7.85(m, 9H). ESI-MS (*m/z*): 295.47 [M+1]. **7i** Full yield 85.8%, mp: 116–118 °C. ¹H NMR (300 MHz, CDCl₃): δ 1.42–1.46(t, 3H, *J* = 7.2 Hz), 4.39–4.47(q, 2H, *J* = 7.2 Hz), 7.26–8.43(m, 7H). ESI-MS (*m/z*): 364.60 [M+1]. **7j** Full yield 75.3%. mp: 126–127 °C. ¹H NMR (300 MHz, CDCl₃): δ 1.42–1.46(t, 3H, *J* = 7.2 Hz), 4.39–4.46(q, 2H, *J* = 7.2 Hz), 7.13–8.22(m, 7H). ESI-MS (*m/z*): 347.89 [M+1]. **7k** Full yield 74.1%. mp: 122–124 °C. ¹H NMR (300 MHz, CDCl₃): δ 1.42–1.47(t, 3H, *J* = 7.2 Hz), 4.40–4.47(q, 2H, *J* = 7.2 Hz), 7.18–8.23(m, 7H). ESI-MS (*m/z*): 393.65 [M+1]. **7n** Full yield 91.0%. mp: 144–146 °C. ¹H NMR (300 MHz, CDCl₃): δ 1.42–1.47(t, 3H, *J* = 7.2 Hz), 4.40–4.48(q, 2H, *J* = 7.2 Hz), 8.47(s, 1H), 7.23–8.60(m, 5H). ESI-MS (*m/z*): 301.37 [M+1].